NAVAL POSTGRADUATE SCHOOL
Monterey, California

THESIS

THEORETICAL INVESTIGATION OF ROTOR ACCELERATION SCHEDULING THROUGH CRITICAL SPEED

by

Cecil C. Bridges

December, 1997

Thesis Advisor: K. T. Millsaps, Jr.

Approved for public release; distribution is unlimited.

1. AGENCY USE ONLY *(Leave blank)*	2. REPORT DATE December 1997	3. REPORT TYPE AND DATES COVERED Master's Thesis	
4. TITLE AND SUBTITLE **THEORETICAL INVESTIGATION OF ROTOR ACCELERATION SCHEDULING THROUGH CRITICAL SPEED.**			5. FUNDING NUMBERS
6. AUTHOR(S) Bridges, Cecil C.			
7. PERFORMING ORGANIZATION NAME(S) AND ADDRESS(ES) Naval Postgraduate School Monterey CA 93943-5000			8. PERFORMING ORGANIZATION REPORT NUMBER
9. SPONSORING/MONITORING AGENCY NAME(S) AND ADDRESS(ES)			10. SPONSORING/MONITORING AGENCY REPORT NUMBER

11. SUPPLEMENTARY NOTES The views expressed in this thesis are those of the author and do not reflect the official policy or position of the Department of Defense or the U.S. Government.

12a. DISTRIBUTION/AVAILABILITY STATEMENT Approved for public release; distribution is unlimited.	12b. DISTRIBUTION CODE

13. ABSTRACT *(maximum 200 words)*

An analytical investigation was conducted to study the amplitude of lateral vibrations and vibrational energy and power of an unbalanced rotor passing through its first lateral bending critical speed. A two degree-of-freedom lumped mass, damping and stiffness model was developed to simulate the response of a simply supported, single disk rotor. Given an arbitrary input acceleration or deceleration, the equations of motion were solved numerically using a fourth order Runge-Kutta routine. The routine used a time step that corresponded to a constant angular phase of rotation. The relationship between the forcing function and lateral vibrational velocity was determined in order to predict the instantaneous power input to the rotor due to the unbalanced rotor. The computer model incorporating an acceleration schedule yielded a result that predicts acceleration scheduling in the location about the critical speed is unable to lower the amplitude of lateral vibrations.

14. SUBJECT TERMS: Accelerating Rotor			15. NUMBER OF PAGES 58
			16. PRICE CODE
17. SECURITY CLASSIFICATION OF REPORT Unclassified	18. SECURITY CLASSIFICATION OF THIS PAGE Unclassified	19. SECURITY CLASSIFICATION OF ABSTRACT Unclassified	20. LIMITATION OF ABSTRACT UL

THEORETICAL INVESTIGATION OF ROTOR ACCELERATION SCHEDULING THROUGH CRITICAL SPEED

Cecil C. Bridges
Lieutenant, United States Navy
B.S., University of Missouri-Rolla, 1988

Submitted in partial fulfillment of the
requirements for the degree of

MASTER OF SCIENCE MECHANICAL ENGINEERING

from the

NAVAL POSTGRADUATE SCHOOL
December, 1997

Author: _____

Cecil C. Bridges

Approved by: _____

Knox T. Millsaps, Jr., Thesis Advisor

_____

Terry R. McNelley, Chairman
Department of Mechanical Engineering

iii

ABSTRACT

An analytical investigation was conducted to study the amplitude of lateral vibrations and vibrational energy and power of an unbalanced rotor passing through its first lateral bending critical speed. A two degree-of-freedom lumped mass, damping and stiffness model was developed to simulate the response of a simply supported, single disk rotor. Given an arbitrary input acceleration or deceleration, the equations of motion were solved numerically using a fourth order Runge-Kutta routine. The routine used a time step that corresponded to a constant angular phase of rotation. The relationship between the forcing function and lateral vibrational velocity was determined in order to predict the instantaneous power input to the rotor due to the unbalanced rotor. The computer model incorporating an acceleration schedule yielded a result that predicts acceleration scheduling in the location about the critical speed is unable to lower the amplitude of lateral vibrations.

TABLE OF CONTENTS

LIST OF SYMBOLS

SYMBOL	DEFINITION (Units, U.S. Customary)
M	Mass of the system. (lbm)
m	Mass of the imbalance.(lbm)
e	Distance form shaft centerline to center of mass imbalance.(in)
x	x displacement of the shaft center. (mils)
y	y displacement of the shaft center. (mils)
R	Magnitude of x and y displacement. (mils)
F	Force. (lbf)
Θ	Angle of eccentric mass. (radians)
$\dot{\Theta}$	Instantaneous angular velocity of the shaft. (rad/sec)
$\ddot{\Theta}$	Instantaneous angular acceleration of the shaft. (rad/sec^2)
Kxx	x direction forces caused by x direction displacement. (lbf/in)
Kyy	y direction forces caused by y direction displacement. (lbf/in)
Kxy	x direction forces caused by y direction displacement. (lbf/in)
Kyx	y direction forces caused by x direction displacement. (lbf/in)
Cxx	x direction forces caused by x direction velocity. (lbf-sec/in)
Cyy	y direction forces caused by y direction velocity. (lbf-sec/in)

Cxy   x direction forces caused by y direction velocity.
                              (lbf-sec/in)

Cyx   y direction forces caused by x direction velocity.
                              (lbf-sec/in)

h   Acceleration of the shaft. $(\text{cycles} / \text{sec}^2)$

t   Time. (seconds)

ζ Damping ratio $(C / 2m\omega_n)$ (1).

I. INTRODUCTION

Rotating machinery is widely used in industrial and military applications. Applications range from gas and steam turbines to electric motors. Rotating shafts have many vibration modes such as axial, torsional and lateral. Lateral vibration is the most important mode of vibration in turbomachine rotors. The lateral vibration is a vibration displacement in the direction perpendicular to the shaft axis.

In many applications of rotating machinery, operation at speeds well above the first or second lateral critical speed is used. The reason is that higher speeds are necessary to achieve high power densities and low lateral vibrations. When equipment is brought to operating speed from rest or when stopping the machinery the critical speed must be crossed. Transition through these critical speeds can induce a large dynamic response in the form of lateral vibrations. The maximum amplitude of these vibrations is responsible for some constraints in the design of rotating equipment. For example, large midspan lateral vibrations may require the designer to use additional tip clearance in turbomachines. The increased tip clearance will in turn reduce the aerodynamic performance of the turbomachine. In addition, the response will create bending stresses and fatigue in the shafting leading to reduced life of the components. Thus, it is crucial that this response be minimized. In addition to the problems of lateral vibrations, energy is transmitted through the bearings to the foundation of the machinery. This energy in turn is radiated through the structure and into the water as acoustic noise. The reduction of this noise is a prime interest to the U.S. Navy in submarine and surface ship silencing.

The response of the rotor as it passes from subcritical to supercritical speed is affected by many factors. These factors include residual imbalance of the rotating shaft, acceleration rate, lubrication fluid forcing within the bearing, method of mounting, bearing type and shaft orientation. Shafts are typically balanced as well as can be practically obtained. However, the response through the critical speed can still cause unacceptable design limitations or severe alternating stresses in the shafting.

The state of the art to reduce lateral vibrations through the critical speed is to accelerate the rotor as fast as possible through the critical speed. This minimizes the time during which the rotor is near its natural frequency and reduces the energy input into the lateral mode of vibration. Increased damping will also assist in lowering the maximum amplitude of the lateral vibrations when passing through the critical speed. The increased damping level can be in excess of the optimum damping for supercritical operation.

Other methods to reduce the lateral vibration through critical speed involve the use of active controls. These methods generally change the shaft or bearing stiffness and thus increase the natural frequency and critical speed. After the rotor is accelerated past the unaided critical speed, the apparatus disengages causing an instantaneous reduction in stiffness in the system. The rotor is suddenly in supercritical operation for the new configuration. The critical speed is crossed without inducing a large dynamic response.

Recent work has shown that acceleration scheduling can lower the maximum amplitude of the lateral vibrations. The concept of acceleration scheduling is that the rotor acceleration is a function of time. The variable acceleration rate is chosen such that it will

2

minimize the lateral vibration response. This is a promising solution in that only the control equipment need be modified in order to implement the acceleration schedule.

The objective of this research is to investigate the how the rate of acceleration affects the lateral vibration response of a rotor as it is accelerated through the first lateral bending critical speed. The knowledge gained through this investigation will then be applied toward predicting an optimum acceleration schedule. Acceleration scheduling has the potential to reduce the maximum amplitude of lateral vibration and to reduce the energy transmitted in the form of lateral vibrations. A computer model along with a numerical solution was used to determine the amplitude and velocity of the vibrating shaft, the power being diverted into lateral vibration and forces generated by the imbalance present in the whirling shaft.

In Chapter II, a brief background is provided on the literature on rotors transiting through critical speed.

In Chapter III, a two degree-of-freedom analytical model is developed for predicting the lateral response of a simple rotor with an arbitrary input acceleration. The ability to change the imbalance of the rotor, damping and stiffness, initial and final RPM, is also included. The equations of motion are explained and method of solution is demonstrated. A free body diagram graphically explains the relation of forces, vibrational velocity and displacement, angular acceleration, velocity and displacement. The results of the model using a constant accelerations are compared to results obtained by Reed [Ref. 1].

In Chapter IV, the results of the modeling and simulation of the rotor shaft are presented. The results are then used to explain the implications on acceleration scheduling.

Conclusions and recommendations are presented in Chapter V.

II. BACKGROUND

The study of the response of an accelerating rotor began in 1932 with Lewis [Ref. 2]. Lewis determined an exact analytical solution of a linearly damped, single degree-of-freedom system accelerated from rest through the first critical speed at a constant acceleration rate. His solution was expressed in terms of Fresnel's integrals. A graphical solution using dimensionless parameters for acceleration, frequency and response analytically was determined and some fundamental aspects of the accelerating rotor were provided. The apparent critical speed is the instantaneous speed of maximum response amplitude. The apparent critical speed will occur at higher speeds and the maximum amplitude will decrease with higher accelerations. Additionally, the apparent critical speed will occur at lower speeds and the maximum amplitude will decrease with increasing deceleration.

In 1933, Pöschl [Ref. 3] and Baker [Ref. 4] in 1939, obtained similar results to those of Lewis.

In 1939, Mueser and Weibel [Ref. 5] extended the analysis to include a generalized solution for the response of a single degree-of-freedom system accelerating through its critical speed. The system incorporated the effects of a cubic nonlinear spring and viscous damping.

In 1949, McCann and Bennett [Ref. 6] analyzed a multi degree-of-freedom system subject to a constant acceleration.

5

In 1965, Filippov [Ref. 7] produced analytical solutions on the vibration response of a linear oscillator using several forcing functions, F(t). A linearly increasing acceleration rate is solved using Lommel's functions. Using similar methods of analysis, he solved for a forcing function amplitude increasing proportionally with frequency squared and decreasing with frequency squared as is the case for an unbalanced rotor.

In 1967, Fearn and Millsaps [Ref. 8] obtained asymptotic approximations for the maximum amplitude and the time at which it occurs for a rotor with constant acceleration or deceleration.

In 1967, Gluse [Ref. 9] investigated the acceleration of a rotor through the critical speed with limited torque. Instead of using a specified constant angular acceleration, he used a constant applied torque. He investigated rotors with limited power supplies and the criteria for the success of a rotor to pass through its critical speed. An unsuccessful acceleration was one in which the rotor was unable to reach supercritical speed. The reason for this failure was that the imbalance of the rotor would cause large lateral deflections. These deflections would develop counter torques opposing the driving torque.

Yamakawa and Murakami [Ref. 10] in 1989, investigated and implemented an optimum design of an operating curve for a two degree-of-freedom rotor system. The work was done with the assumption that the rotor would have a limited power supply and thus a maximum applied torque. A gradient-based optimization method was used to determine the operating curve as to minimize the dynamic response about the critical speed. The main difference between their model and the one developed in Chapter III is

6

the limitation of available torque. The model developed assumes that the motor driving the rotor is able to maintain the maximum acceleration at all speeds. Additionally, their model did not use cross-stiffness or cross-damping. The operating curve was then applied through a motor controller to a rotor kit. From the experimental evidence a 30% reduction of the maximum lateral vibration amplitude was obtained.

In 1995, Reed [Ref. 1] developed a two degree-of-freedom, planar, lumped mass damping and stiffness analytical model. Different acceleration rates, asymmetric damping, and asymmetric stiffness were implemented in the model to predict the rotordynamic response. He then used an experimental rotor facility to verify the effect of the different acceleration rates on the maximum amplitude of the lateral vibrations. He also conducted an investigation into a simple acceleration schedule. In his acceleration schedule, the rotor is accelerated from an initial speed to a speed below the apparent critical speed of that acceleration rate. The apparent critical speed is the speed at which that acceleration rate produces the maximum amplitude. It occurs at a higher speed than that of the steady state critical speed. The acceleration is switched from the high acceleration rate to a lower rate of acceleration. The results of his model showed that the amplitude of the response was only slightly less than that obtained by maintaining the high acceleration. The benefit of this schedule was that the response would " ring down" much faster than the constant high acceleration curve and inflict fewer high lateral vibration cycles about the apparent critical frequency.

In 1996, Milsaps and Reed [Ref. 11] conducted work on the use of acceleration scheduling to reduce lateral vibrations of a rotor passing through critical speeds. This was

7

a continuation of the work conducted by Reed on acceleration scheduling. In this paper, the High/Low schedule was implemented on the rotor test facility to experimentally verify the effect of the acceleration schedule. They obtained a 12% reduction in lateral vibrations using a simple acceleration schedule. They deduced that an even greater reduction in lateral vibrations might be possible with an optimum acceleration schedule.

Currently, it is known that the reduction of the maximum amplitude of lateral vibrations is achievable by increasing the acceleration rate and that by increasing the acceleration rate, the apparent critical frequency will shift to a higher speed. The research conducted by Millsaps and Reed [Ref. 11] suggest that a simple high/low acceleration schedule will also reduce the amplitude of the response. Yamakawa and Murakami [Ref. 10] determined that an optimum rotor acceleration schedule is obtainable for limited power systems.

It is not known if there is an optimum solution that will reduce the maximum amplitude of lateral vibrations. The status of the rotor between the lower acceleration apparent critical speed and the higher acceleration apparent critical speed needs to be determined. This will help to explain why acceleration scheduling works and how the schedule can be optimized. Lastly, the behavior of the rotor as the acceleration rate is changed needs to be better understood.

III. ANALYTICAL MODEL

A.   MODEL DEVELOPMENT

In order to predict the rotordynamic response of a rotor transiting from subcritical to supercritical, an analytical model was developed. The rotor is characterized as a two degree-of-freedom, lumped mass and stiffness with direct stiffness and damping as shown in Figure 1. In addition cross-stiffness and cross-damping terms are included. The stiffness and damping of the shaft, bearings, and support structure are combined into single terms Kxx, Kyy, Kxy, Kyx, Cxx, Cyy, Cxy and Cyx. The model assumes that the two bearings supporting the shaft are identical.

The equations of motion for the rotor and disk model system are as follows:

$$M\ddot{x} + C_{xx}\dot{x} + C_{xy}\dot{y} + K_{xx}x + K_{xy}y = me(\ddot{\Theta}\cos\Theta - \dot{\Theta}^2\sin\Theta). \qquad (1)$$

$$M\ddot{y} + C_{yy}\dot{y} + C_{yx}\dot{x} + K_{yy}y + K_{yx}x = me(\ddot{\Theta}\sin\Theta + \dot{\Theta}^2\cos\Theta). \qquad (2)$$

The total modal mass of the system is denoted as M. This is obtained by assuming the mode shape of the shaft to be the same as a pinned-pinned beam. The mass imbalance is m, at a distance e, from the center of the shaft. This distance is fixed for the model. The angular displacement theta, Θ, is a prescribed function of time. This angle is measured from the y-axis as the disk and shaft rotates about the shaft center.
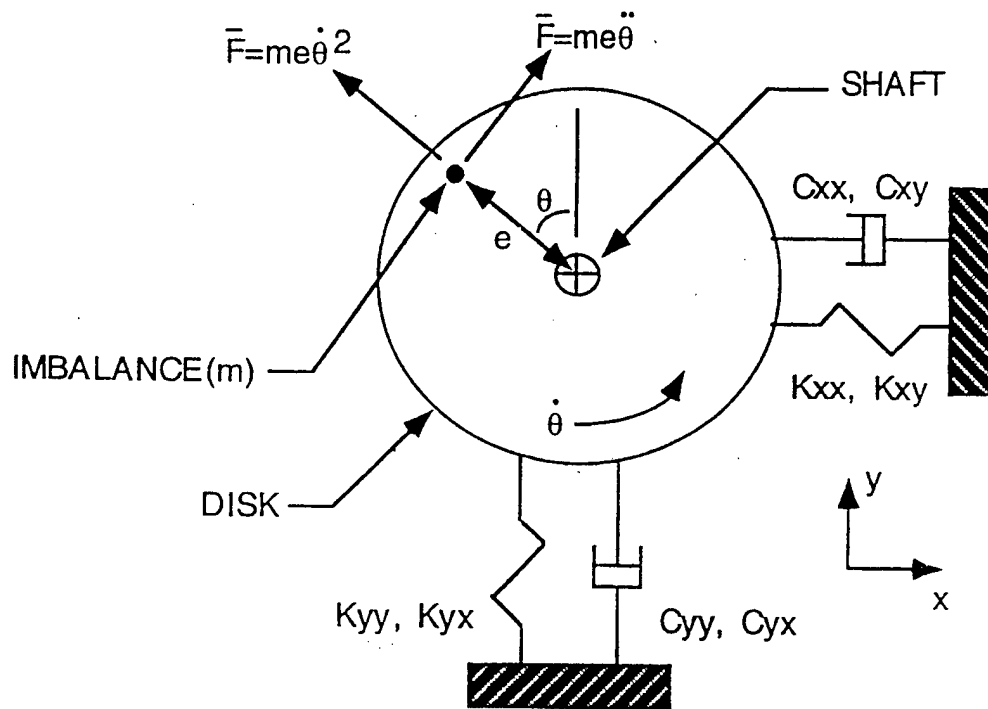
Figure 1. Analytic Lumped Mass and Stiffness Model of a Two Degree-of-Freedom Rotating Shaft and Disk Assembly with Direct and Cross-Coupled Linear Stiffness and Damping.

The equations of motion can also be written in the matrix form as follows:

$$\begin{bmatrix} M & 0 \\ 0 & M \end{bmatrix}\begin{Bmatrix} \ddot{x} \\ \ddot{y} \end{Bmatrix} + \begin{bmatrix} Cxx & Cxy \\ Cyx & Cyy \end{bmatrix}\begin{Bmatrix} \dot{x} \\ \dot{y} \end{Bmatrix} + \begin{bmatrix} Kxx & Kxy \\ Kyx & Kyy \end{bmatrix}\begin{Bmatrix} x \\ y \end{Bmatrix} = me\begin{Bmatrix} \ddot{\Theta}\cos\Theta - \dot{\Theta}^2\sin\Theta \\ \ddot{\Theta}\sin\Theta + \dot{\Theta}^2\cos\Theta \end{Bmatrix} \quad (3)$$

B. SOLUTION TECHNIQUE

The equations of motion were solved numerically using a fourth order Runge-Kutta method. The two second order differential equations are broken down into four first order equations as follows:

$$\dot{x}_2 = \left(\frac{me}{M}\right)\left(\ddot{\Theta}\cos\Theta - \dot{\Theta}^2\sin\Theta\right) - \left(\frac{Cxx}{M}\right)x_2 - \left(\frac{Cxy}{M}\right)y_2 - \left(\frac{Kxx}{M}\right)x_1 - \left(\frac{Kxy}{M}\right)y_1 \quad (4)$$

$$\dot{x}_1 = x_2$$

$$(5)$$

$$\dot{y}_2 = \left(\frac{me}{M}\right)\left(\ddot{\Theta}\sin\Theta + \dot{\Theta}^2\cos\Theta\right) - \left(\frac{Cyy}{M}\right)y_2 - \left(\frac{Cyx}{M}\right)x_2 - \left(\frac{Kyy}{M}\right)y_1 - \left(\frac{Kyx}{M}\right)x_1 \quad (6)$$

$$\dot{y}_1 = y_2$$

$$(7)$$

A variable time step corresponding to a constant phase or angular displacement interval of the rotating disk was used for the calculation. This was done in order for predictions from the model to be matched directly with the data points taken from the lab facility. For the experimental rotor, the (x-y) displacement data are taken with an optical encoder. The optical encoder acquires data at a constant angular phase. Four initial

11

conditions are needed to fully describe the state of the rotor system. These are x and y displacement and velocity in the x and y direction. These initial conditions of the program could be taken from either a steady-state solution or conditions from a previous time step at any acceleration.

1. Radial Displacement

The model was used to predict the x and y displacement of the rotor shaft center as a function of time. The amplitude of this displacement is given by:

$$R(t) = \sqrt{x^2(t)+y^2(t)} \qquad (8)$$
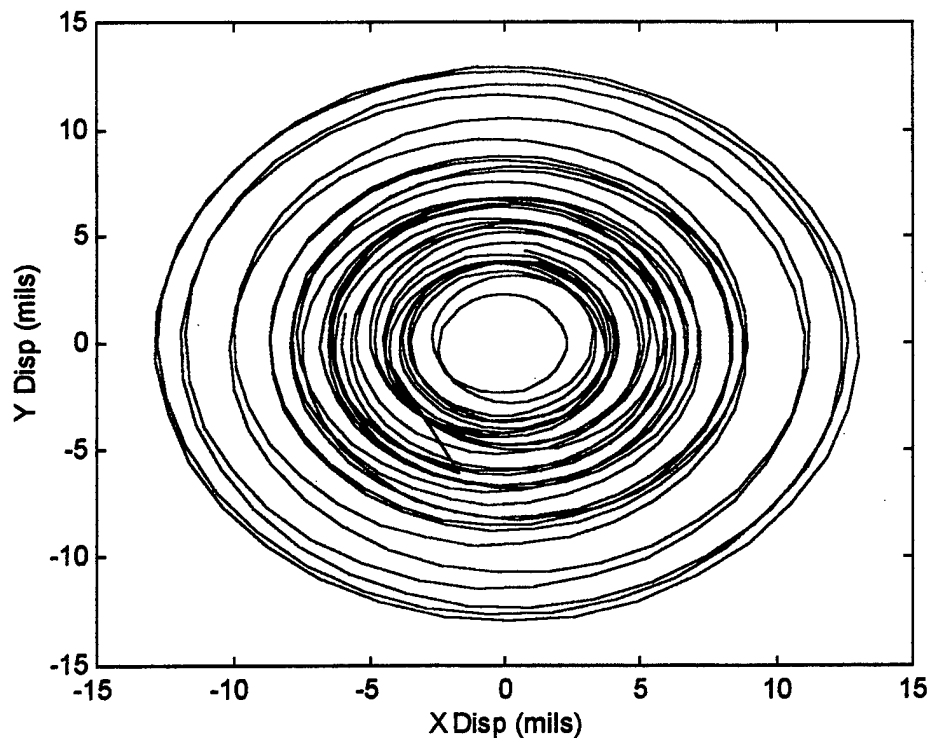
Figure 2 shows the typical resulting orbits of R(t).

Figure 2. Rotor Orbits from the Model Calculated Using a Constant Phase Time Step.

12

2. Phase Angle of the Mass Imbalance

In order to fully describe the condition of the rotor system, the relative position of the mass imbalance to the (x-y) motion of the center of the bearings must be described. This is shown in Figure 3. During steady-state, low subcritical speeds the imbalance will remain "heavy side out". The mass imbalance is in the same phase as the radial displacement vector. At the steady state critical speed, the response lags the forcing by 90°. At high supercritical speeds, the response lags the forcing by 180°. This condition is known as "heavy side in".
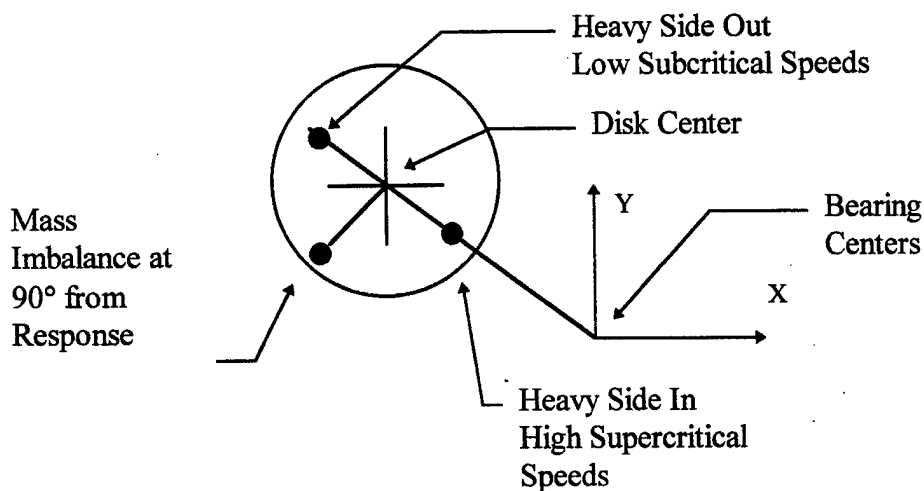

Figure 3. The Relationship Between the Mass Imbalance and Radial Displacement R(t) for Steady State Subcritical, Critical and Supercritical Speeds.

C. POWER AND ENERGY CONSIDERATIONS

The maximum amplitude of radial displacement, R(t), is dependant upon the energy fed into the rotor's lateral vibration. The energy for lateral vibration is drawn from the rotational energy of the spinning shaft by the eccentric whirling mass, m. The energy is removed by damping and energy transfer back into the rotational energy of the shaft. The input power to the shaft due to the applied torque, T, is given by Equation 9.

$$Pin = T\omega \qquad (9)$$

ω is the instantaneous angular velocity. The total energy of the system in the shaft is the sum of the rotational kinetic energy of the disk, Er, and the kinetic and potential energy of the lateral vibration, Et. These are given by Equations 11 and 12 respectively.

$$Er = \frac{1}{2} Izz\omega^2 \qquad (10)$$

$$Et = \frac{1}{2} M(\dot{x}^2 + \dot{y}^2) + \frac{1}{2} K(x^2 + y^2) \qquad (11)$$

The polar moment of inertia is given by Izz. The power transfer to and from the lateral vibration is given by the following equation:

$$Power\ transfer = \vec{F}(t) \bullet \vec{V}(t) = |F||V| \cos \Theta_1 \qquad (12)$$

The vector F(t) represents the force as a result of the radial and tangential acceleration of the eccentric mass. The vector V(t) is the velocity of the center of the shaft with respect to the bearing centers.

14

This relationship is shown in Figure 4. The angle Θ_1 is the angle between the vectors F(t) and V(t). The magnitude of the velocity V(t) is given by:

$$\left| V(t) \right| = \sqrt{\dot{x}^2(t) + \dot{y}^2(t)} \tag{13}$$
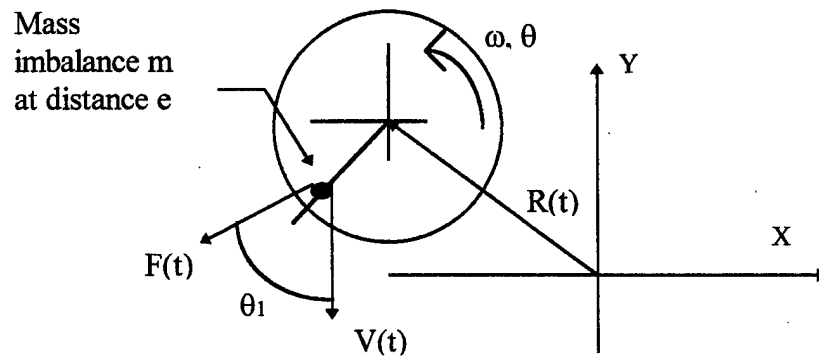

Figure 4. Model Diagram Showing the Relationship Between F(t) and V(t).

If the angle, Θ_1, is greater than $\pi / 2$, the power transfer will be negative. The power is leaving the lateral mode of vibration and going into the rotational power of the shaft. This condition will result in R(t) decreasing as the vibrational kinetic and potential energy is decreasing.

D. MODEL VALIDATION

The computer model is similar to the one produced by Reed [Ref.1] with the exception that he used the MATLAB utility of ODE45 with a time step provided by that program. His results were verified against the analytical results of Lewis [Ref. 2] and by comparing the results obtained for a very low acceleration rate to steady state results. The constant phase solution yields results identical to Reed's. Therefore, it can safely be assumed that the constant phase integration method yields accurate results.

IV. DISCUSSION OF MODEL RESULTS

A. MODEL RESULTS

1. Introduction

To analyze the rotordynamic response of a rotor undergoing acceleration through its critical speed three simulations were conducted. Acceleration rates are compared using a dimensionless number q, given by:

$$q = \frac{\omega_n^2}{h} \tag{14}$$

Where h is the acceleration rate in cycles per second^2 and ω_n is the natural frequency of the system in cycles per second. The numerical value of q corresponds to the number of cycles from 0 to ω_n.

The response of a low acceleration of 250 RPM/second (q=493) was compared to the response at a high acceleration rate of 2000 RPM/second (q=62). These are the upper and lower accelerations that were considered for the acceleration scheduling. The last scenario is the result of the proposed acceleration schedule in which the high acceleration is switched to the low acceleration prior to the apparent critical speed of the higher acceleration. All plots are have both time and RPM scales to describe the behavior of the rotor.

The rotordynamic coefficients were chosen to match the steady state response of the experimental facility. These are shown in Table 1 in the Appendix.

2. 250 RPM/Second Constant Acceleration Rate

a. Radial Displacement

The lateral vibration response for the 250 RPM/second constant acceleration rate is shown in Figure 5. The maximum amplitude of lateral vibrations occurs at 2790 RPM. Figure 6 is the angular difference between the XY center of mass of the disk vector angle and the angle the rotor has turned. The XY center of mass angle is determined by the position of the rotor about the bearing centers. The angle the rotor has turned is determined by the acceleration of the rotor. This angular difference is used to determine the relative phase of the mass imbalance. From Figure 6, the mass imbalance is at 0° while the rotor is far below the critical speed, the "heavy side out" condition. As the rotor approaches the critical speed, the mass imbalance will undergo a rotation to 180° out of phase with the response vector. This is the "heavy side in" condition. The lateral vibration response will rise and fall in step with the oscillation of the angular difference about 180° in the supercritical region.

b. Vibrational Power Transfer

The vibrational power transfer plots are shown in Figure 7. The periods where power transfer is positive indicates that the forcing due to the mass imbalance is providing power to the lateral vibration. For negative power transfer, the force due to the mass imbalance is removing power from the lateral vibration. Comparing Figure 7 to Figure 5, the periods of increasing response coincide with periods of power transfer greater than zero. The maximum amplitude of power transfer lags behind the maximum amplitude for response by about 10 RPM. Figure 8 is a plot of the angle used to compute

18

the lateral vibrational power. From Equation 12, the dot product of the two vectors will be zero when the angular difference is 90° or 270°. At the speed or time when the angle in Figure 8 is 90°, the power transfer will change from positive to negative. The power transfer will fluctuate about zero when the angular difference oscillates about 90° in the supercritical region.

3.   **2000 RPM/Second Constant Acceleration Rate**

a.   **Radial Displacement**

The radial displacement R(t), for the 2,000 RPM/second constant acceleration rate is shown in Figure 9. The maximum amplitude of lateral vibrations occurs at 2,990 RPM. Figure 10 is the angular difference between the XY center of mass of the disk vector angle and the angle the rotor has turned. From Figure 10, the mass imbalance is at 0° while the rotor is far below the critical speed, the "heavy side out" condition. In the range of rotor speeds above the critical speed the mass imbalance continues to rotate about the XY center of mass. The phase between the response and the imbalance does approach (-180°) in an oscillatory manner at speeds far in excess of the apparent critical speed. The continued rotation explains the supercritical fluctuations in R(t).

b.   **Vibrational Power Transfer**

The vibrational power transfer plots are shown in Figure 11. Comparing Figure 11 to Figure 9, the periods of increasing response coincide with periods of positive power transfer. The power exhibits rapid fluctuations about zero as the speed increases beyond the critical speed. The maximum amplitude of power transfer leads the

maximum amplitude for response by about 90 RPM. Figure 12 is a plot of the angle used to compute the power transfer. The power transfer begins to fluctuate about zero when the angular difference oscillates about -90° in the far supercritical region.

4.   Acceleration Schedule, 2000 to 250 RPM/Second

a. Introduction

The previous work of Reed [Ref. 1] and Millsaps and Reed [Ref. 11] concluded that it was possible to switch from a high acceleration to a low acceleration to reduce the maximum amplitude of lateral vibrations. This concept is known as acceleration scheduling. The high/low switching method is also known in optimization text as the "Bang-Bang" or "Bang-Off-Bang" solution. This simple but useful optimization technique is also employed in planning the trajectories of rockets in order to obtain an optimum fuel consumption rate. The Bang-Off-Bang solution means that the maximum energy or power is put forth until a certain time then the power or energy level is switched to a lower energy level for a "lull" period. After which the power or energy is switched back to the higher level.

The supporting hypothesis behind this high/low acceleration schedule is to take advantage of the shift of the apparent critical speeds. As previously discussed, a constant acceleration will cause the apparent critical speed to shift toward the right and thus occurring at higher speeds. The rotor would be accelerated from a subcritical speed using the high acceleration rate. Once past the apparent critical speed of the lower acceleration rate, at the speed near where the two radial displacement curves intersect, the acceleration rate is switched. It is believed that the rotor will respond as if it is suddenly

20

supercritical and drive toward the response of the lower acceleration thus producing a maximum amplitude of lateral vibration at the switching speed.

b. Radial Displacement

The acceleration schedule is presented in Figure 13. The acceleration rate is switched when the high acceleration rate intersects the low acceleration rate as shown in Figure 14. With the desired response, a 25% to 30% decrease in the maximum radial displacement is possible. Figure 15 shows that no improvement is made by switching the acceleration rates. The maximum response is slightly above the 10 mils response of the 2000 RPM/second constant acceleration rate. The maximum occurs at a lower apparent critical speed than the 2000 RPM/second constant acceleration rate. In addition, the response diminishes similar to the 250 RPM/second constant acceleration rate. Figure 16 is the angular difference between the XY center of mass of the disk vector angle and the angle the rotor has turned. The imbalance begins at zero and ascends to 100° at the switch. From the time plot of Figure 16, after the switch the imbalance rotation changes from a parabolic increase to a nearly linear increase. Upon crossing the apparent critical speed the imbalance oscillates about 180°.

c. Vibrational Power Transfer

The vibrational power transfer plots are shown in Figure 17. After the switch, the power transfer drops rapidly with respect to RPM. The time plot in Figure 17, shows that the power decreases at the same rate of increase prior to the apparent critical speed. The maximum amplitude of power transfer lags behind of the maximum amplitude for radial displacement by 10 RPM. Figure 18 is a plot of the angle used to compute the

21

power transfer. The power transfer fluctuates about zero when the angular difference oscillates about -90° in the far supercritical region.

5. Comparison of Constant High Acceleration to Acceleration Schedule

The computer model revealed that acceleration scheduling near the first critical speed did not reduce the maximum amplitude of radial displacement. The reason for the inability for the rotor to execute the response path of the lower acceleration lies in the rotation of the mass imbalance. When the acceleration was switched from high to low, the mass imbalance was at 100°, upon switching the imbalance rotated to 180° and oscillated about this value while the response diminished. After the switch the response increased to 10.4 mils.

A comparison of the high acceleration rate and the acceleration schedule radial displacement is shown in Figures 19 and 20. In Figure 19, the two responses are plotted against RPM. In Figure 20, the two responses are plotted against time. After the apparent critical speed is past, the mean radial displacement of the 2000/250 RPM/second acceleration schedule is 2.05 mils. The supercritical mean radial displacement of the 2000 RPM/second constant acceleration is 5.43 mils.

Reed [Ref. 1] using the same model obtained results that suggested that acceleration scheduling is possible. His results indicate the response will decrease rapidly after the switch but due to high amplitude transients present in the decreasing response, the maximum amplitude is only slightly less than that of the constant 2000 RPM/second response. From experience with the computer model during the research, this type of solution could be caused by improperly prescribing the rotor conditions when switching to

22

a lower acceleration.

In the analysis, the conditions of the stiffness and damping were kept symmetric and the cross-stiffness and cross-damping terms were set to zero. This simplification was necessary to isolate and study the effects of acceleration scheduling on the vibrational power, energy and the rotation of the mass imbalance. With these parameters present the solution would be more complicated. The effects of these factors on the lateral bending response was determined in detail by Reed [Ref. 1].
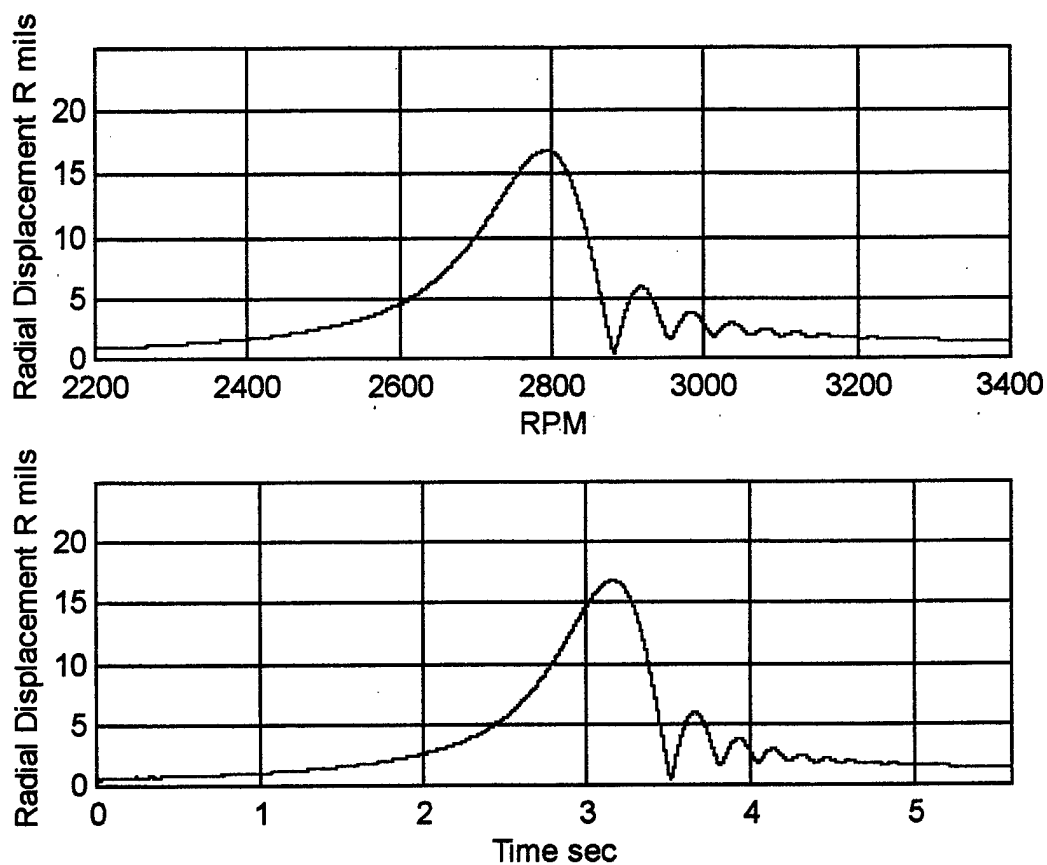
Figure 5. Vibrational Radial Displacement of an Accelerating Rotor.
(All Cross Terms are Zero, Kxx=Kyy=495 lbf/in,Cxx=Cyy=0.04 lbf-sec/in, Acceleration rate 250 RPM/Sec).

24
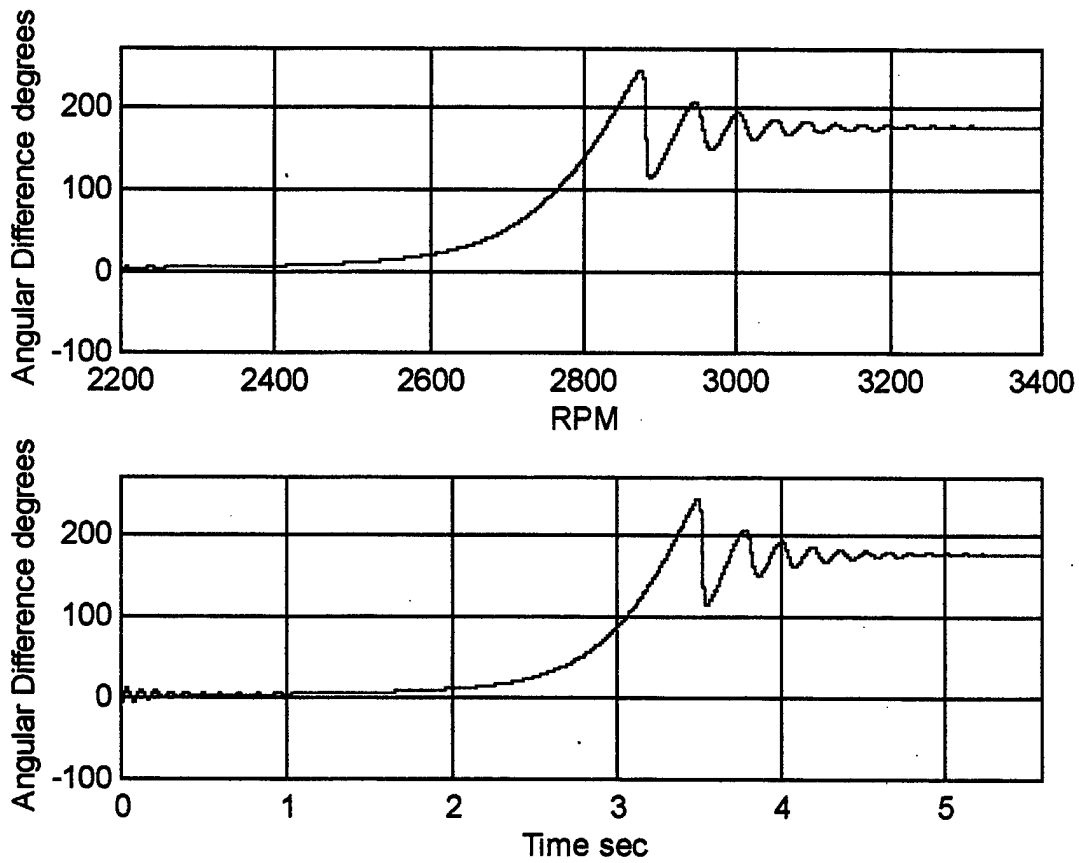
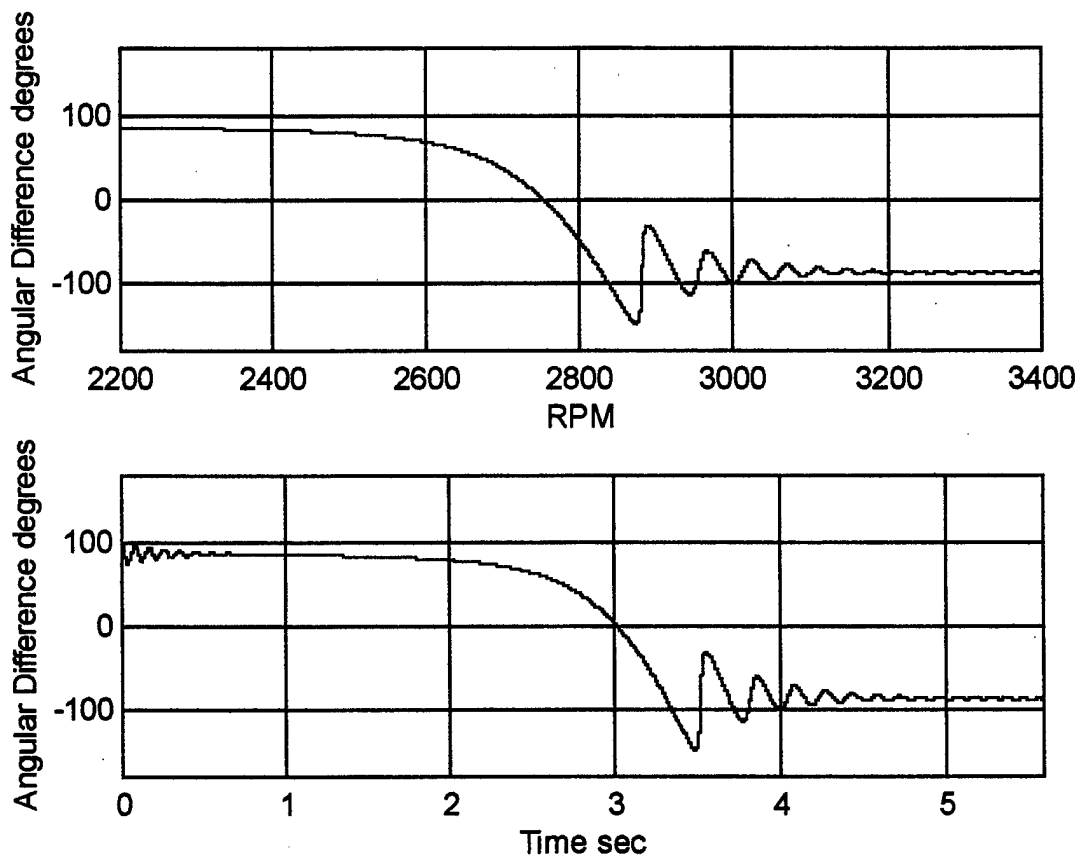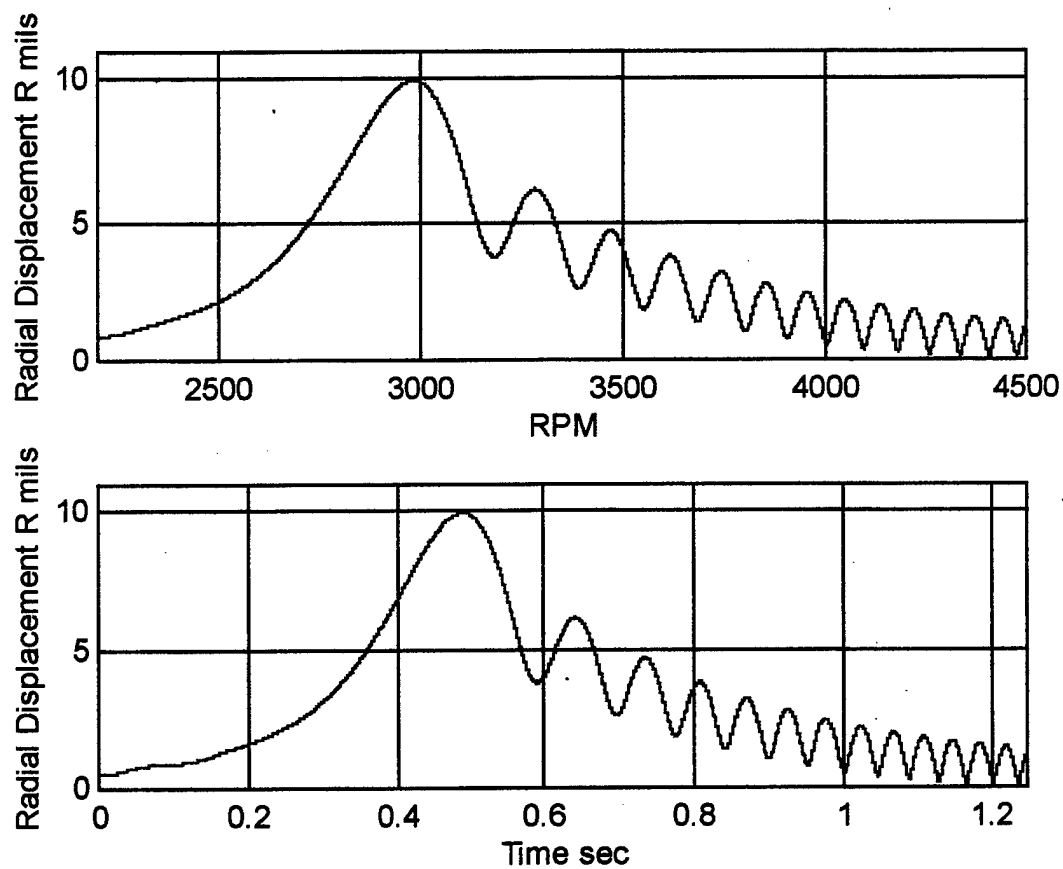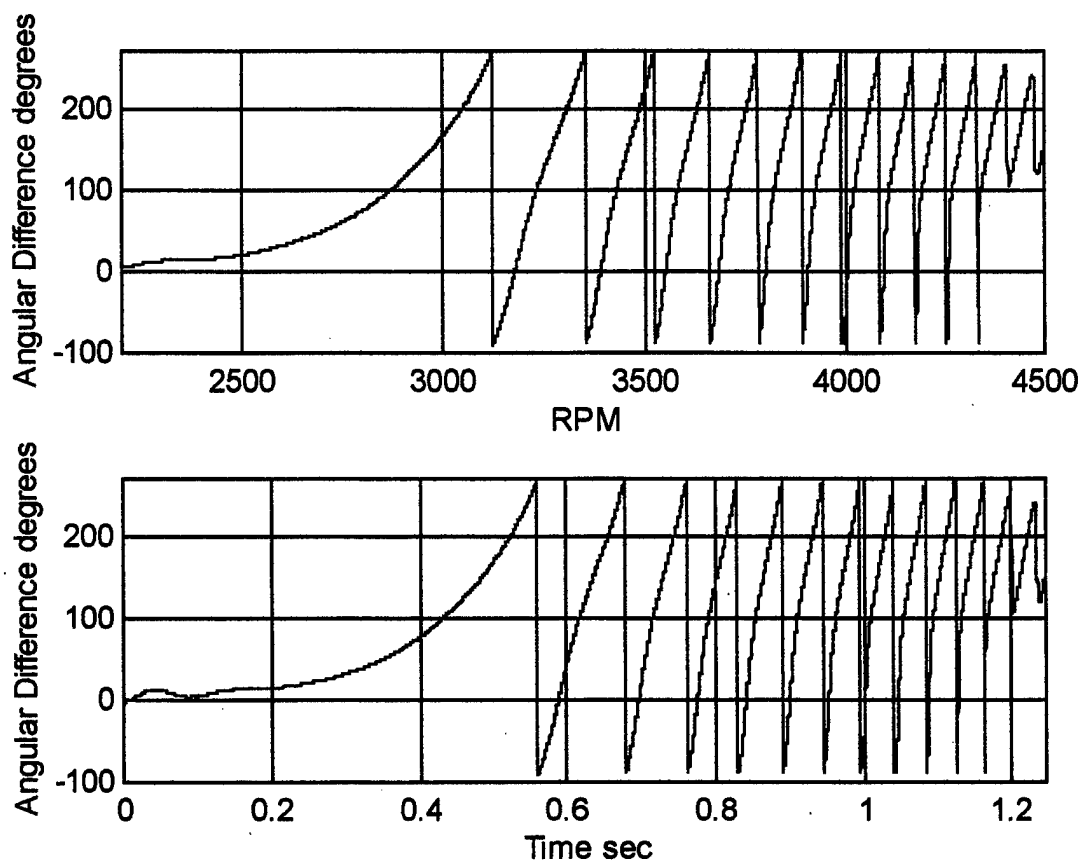**Figure 6. Angle Between the XY Center of Mass and Angular Displacement (Θ) of an Accelerating Rotor. (All Cross Terms are Zero, Kxx=Kyy=496 lbf/in,Cxx=Cyy=0.04 lbf-sec/in, Acceleration rate 250 RPM/Sec).**

25
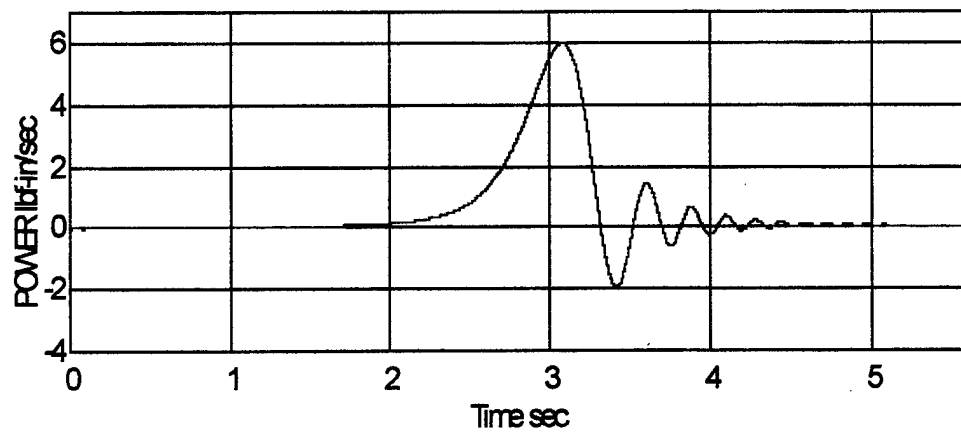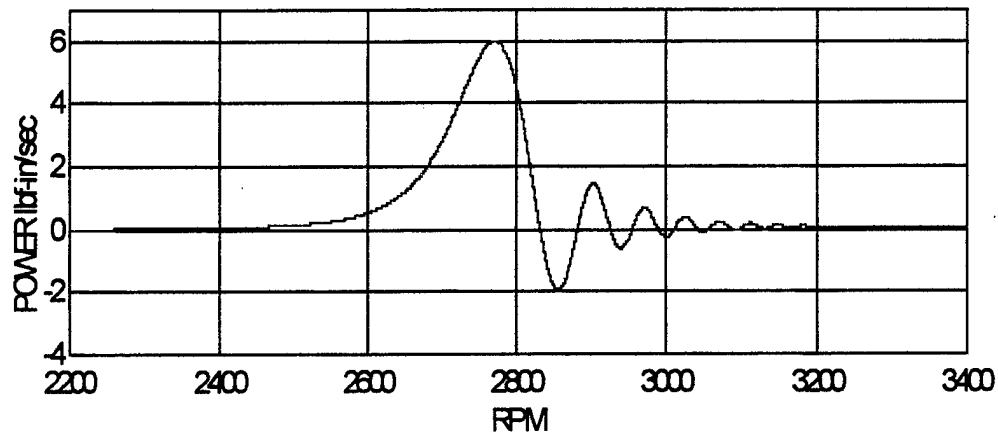
Figure 7. Vibrational Power Transfer of an Accelerating Rotor.
(All Cross Terms are Zero, Kxx=Kyy=495 lbf/in,Cxx=Cyy=0.04 lbf-sec/in,
Acceleration rate 250 RPM/Sec).

26

Figure 8. Angle Between Force and Velocity Vectors of an Accelerating Rotor.
(All Cross Terms are Zero, Kxx=Kyy=495 lbf/in,Cxx=Cyy=0.04 lbf-sec/in, Acceleration
rate 250 RPM/Sec).

27

Figure 9. Vibrational Radial Displacement of an Accelerating Rotor.
(All Cross Terms are Zero, Kxx=Kyy=495 lbf/in,Cxx=Cyy=0.04 lbf-sec/in, Acceleration
rate 2000 RPM/Sec).

28

Figure 10. Angle Between the XY Center of Mass and Angular Displacement (Θ) of an Accelerating Rotor. (All Cross Terms are Zero, Kxx=Kyy=495 lbf/in,Cxx=Cyy=0.04 lbf-sec/in, Acceleration rate 2000 RPM/Sec).
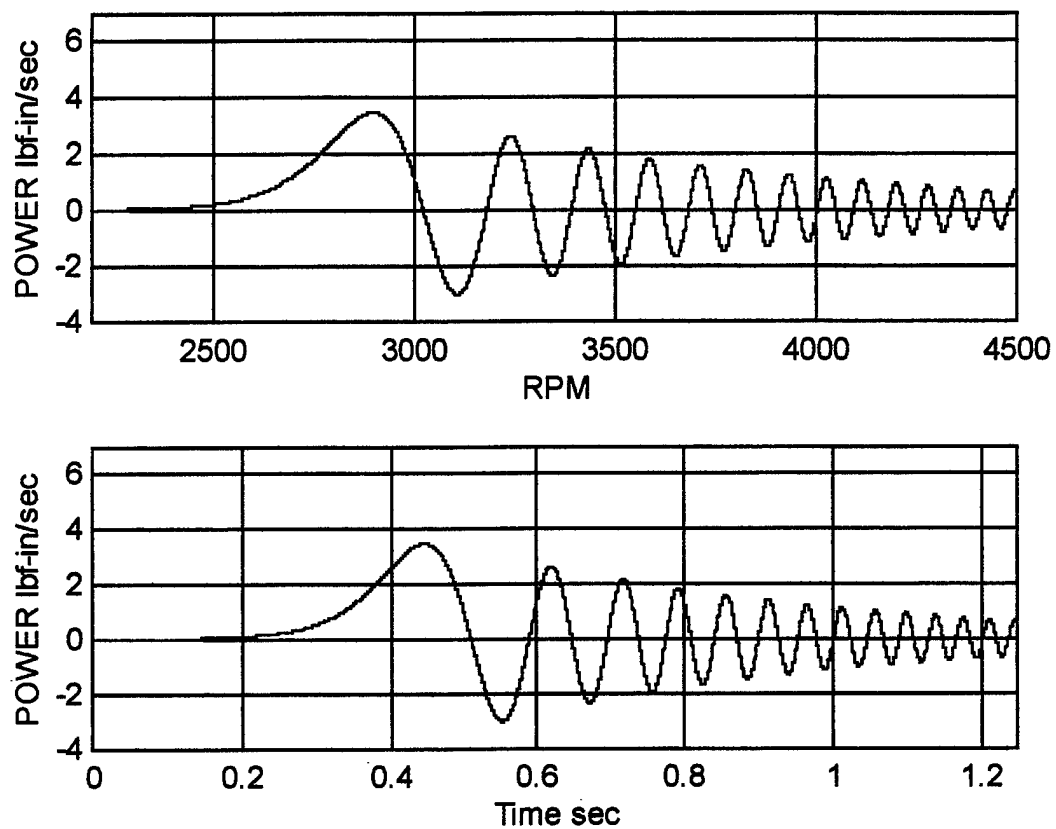
**Figure 11. Vibrational Power Transfer of an Accelerating Rotor.
(All Cross Terms are Zero, Kxx=Kyy=495 lbf/in,Cxx=Cyy=0.04 lbf-sec/in, Acceleration
rate 2000 RPM/Sec).**

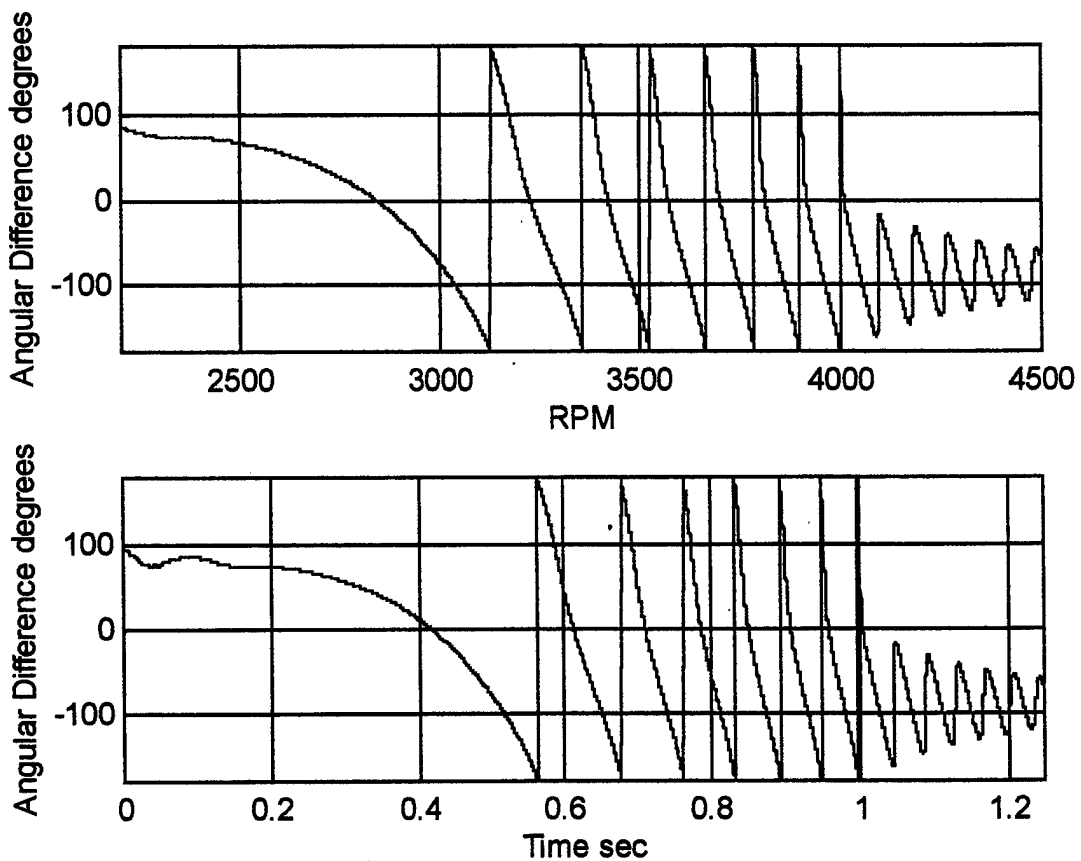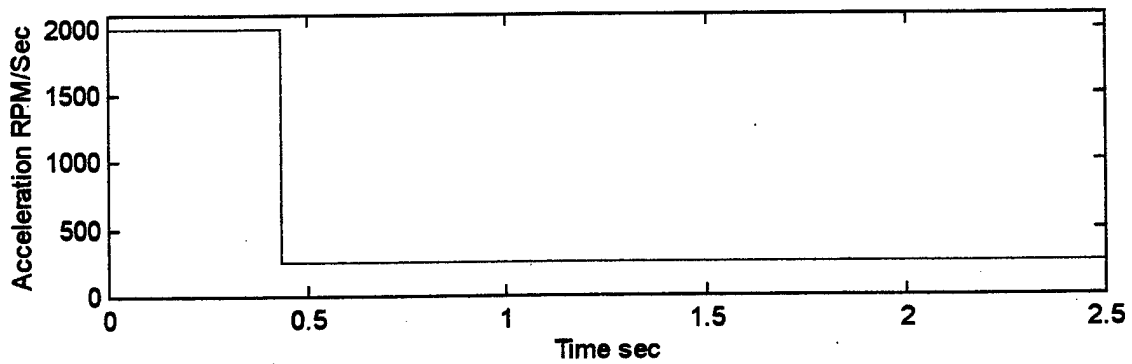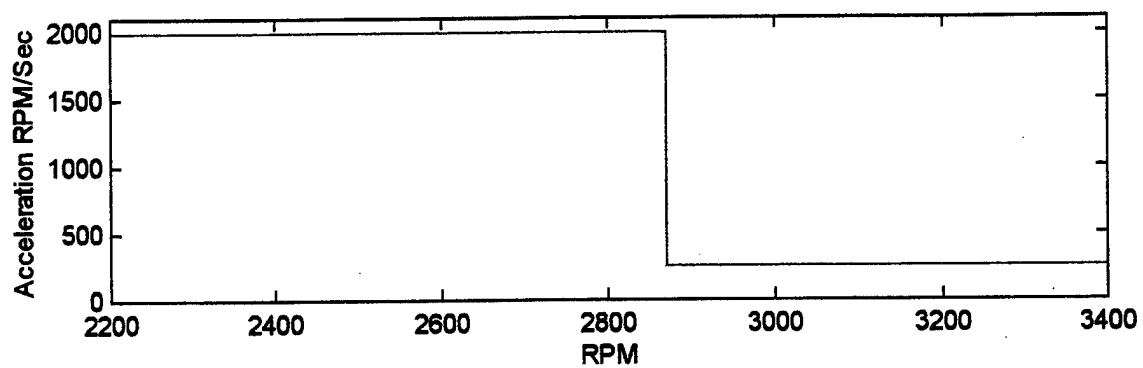Figure 12. Angle Between Force and Velocity Vectors of an Accelerating Rotor.
(All Cross Terms are Zero, Kxx=Kyy=495 lbf/in,Cxx=Cyy=0.04 lbf-sec/in, Acceleration
rate 2000 RPM/Sec).

**Figure 13 . Angular Acceleration Schedule of the Rotor.
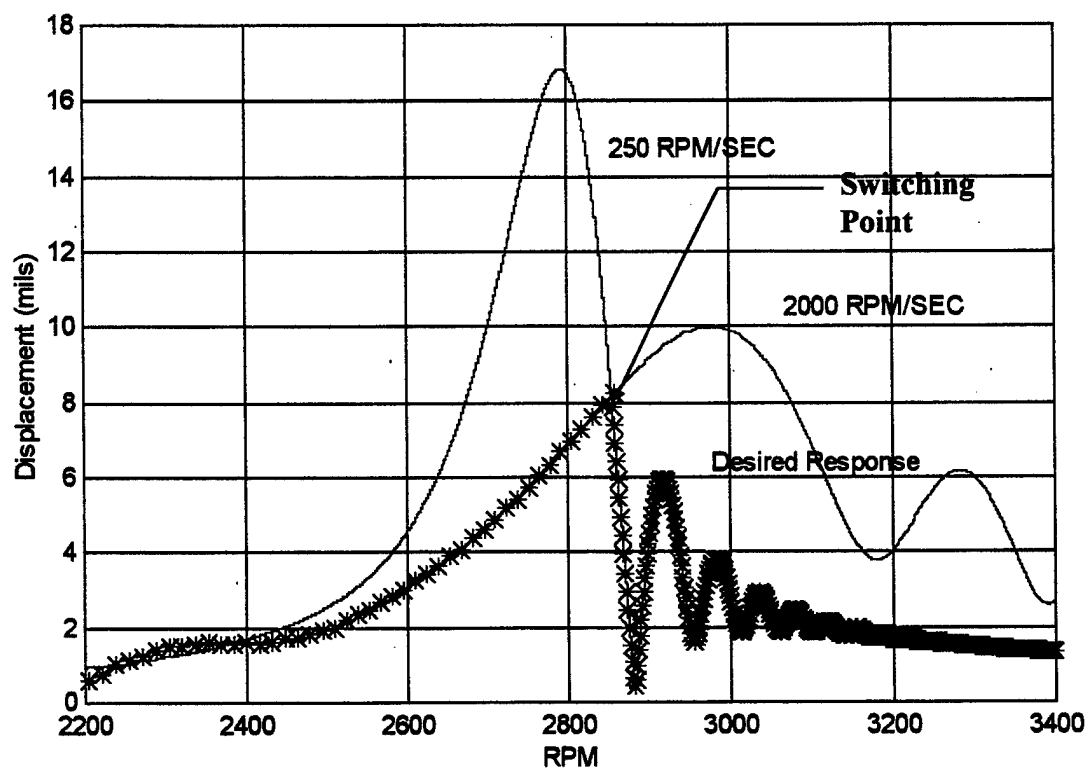Acceleration Schedule 2000 to 250 RPM/Sec at 2870 RPM**

Figure 14. Representation of how the Shift in the Apparent Critical Speed may be used to reduce Maximum Rotor Response.
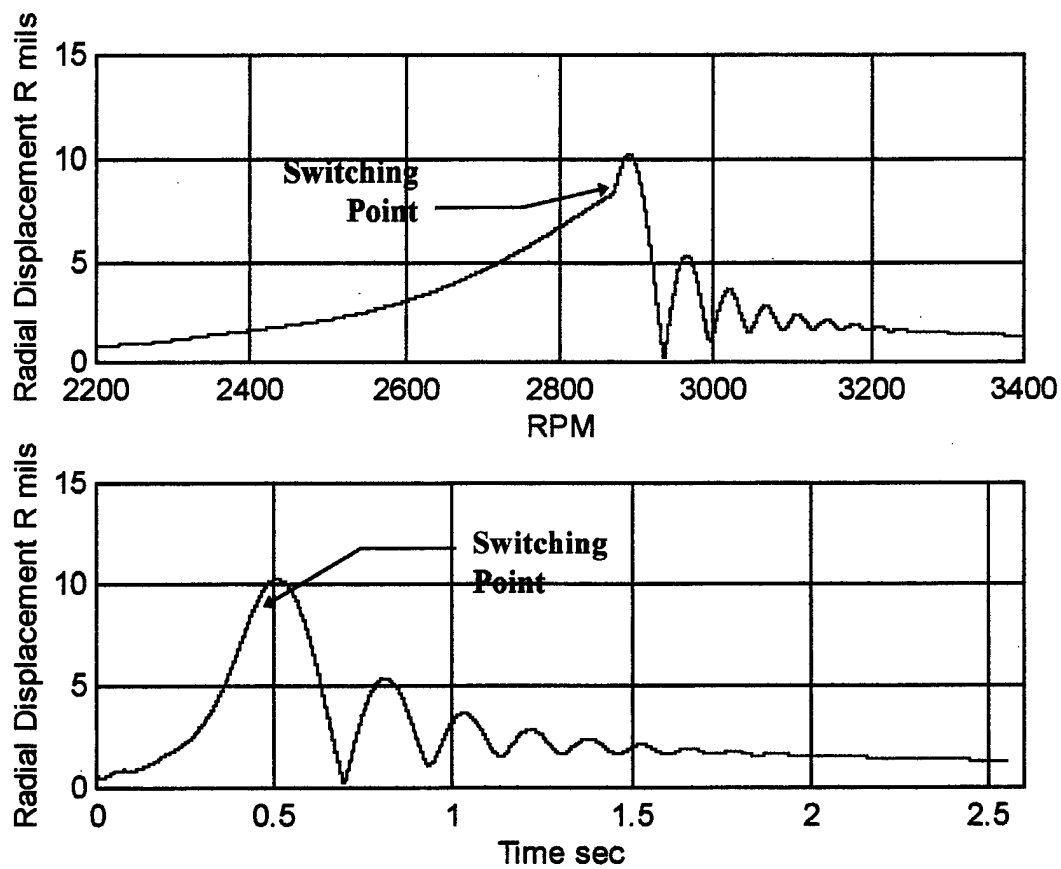
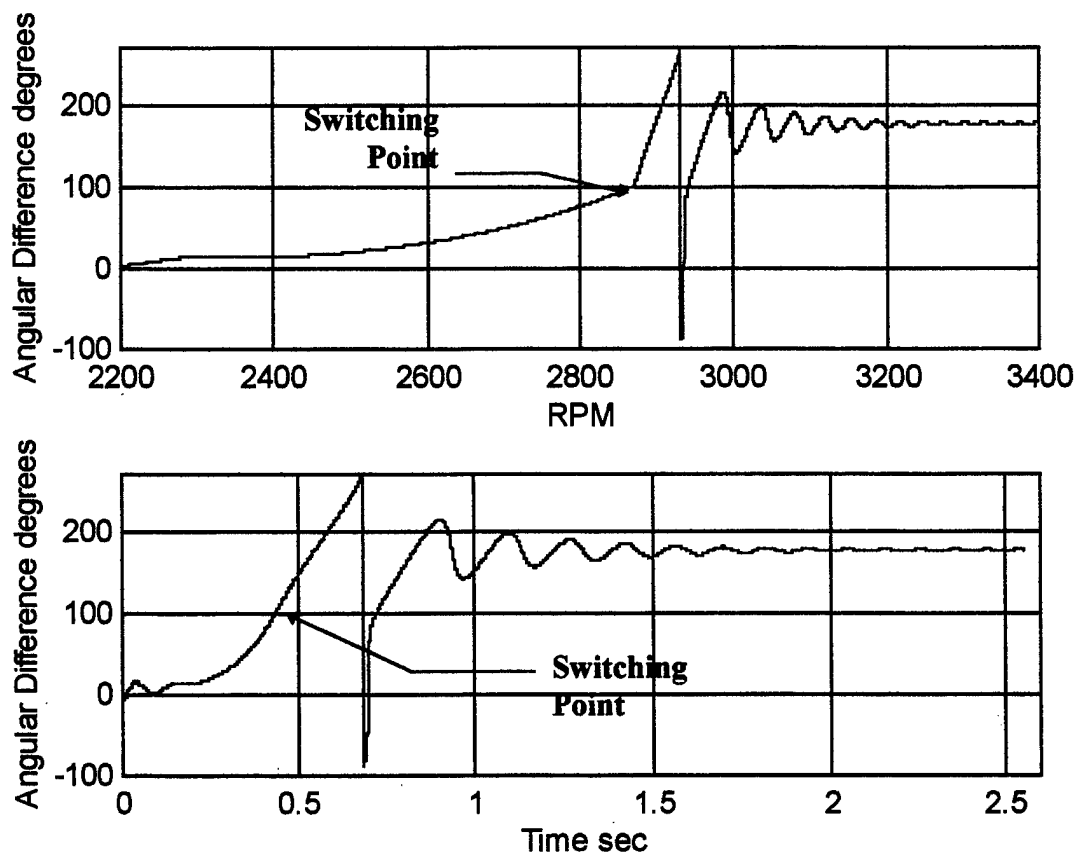Figure 15. Vibrational Radial Displacement of a Rotor.
Acceleration Schedule 2000 to 250 RPM/Sec at 2870 RPM
(All Cross Terms are Zero, Kxx=Kyy=495 lbf/in,Cxx=Cyy=0.04 lbf-sec/in).

Figure 16. Angle Between the XY Center of Mass and Angular Displacement (Θ) of a Rotor. Acceleration Schedule 2000 to 250 RPM/Sec at 2870 RPM (All Cross Terms are Zero, Kxx=Kyy=495 lbf/in,Cxx=Cyy=0.04 lbf-sec/in).
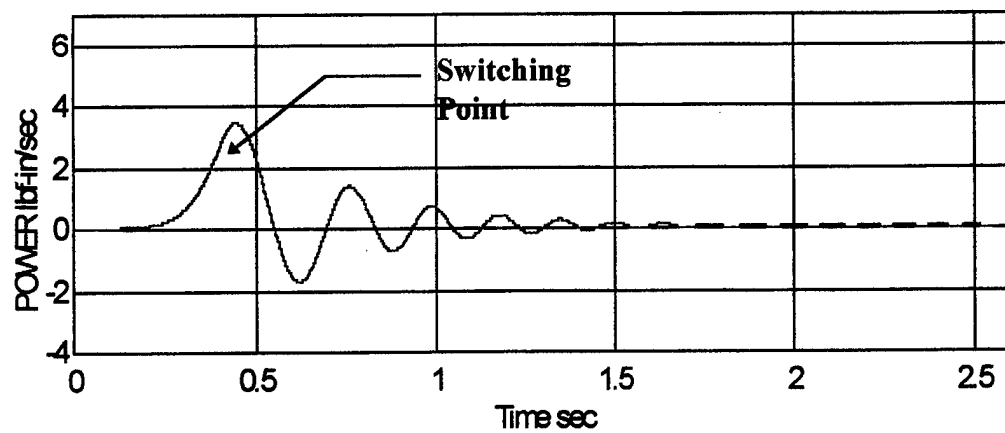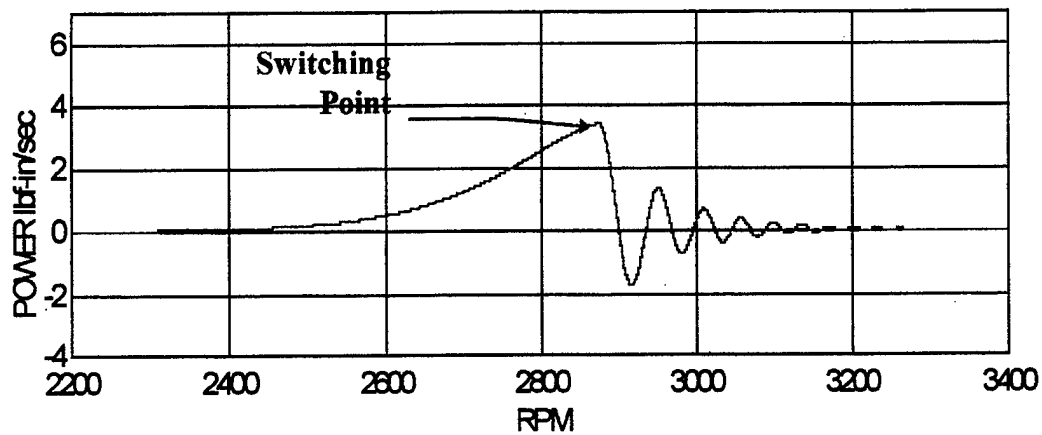
Figure 17. Vibrational Power Transfer of a Rotor.
Acceleration Schedule 2000 to 250 RPM/Sec at 2870 RPM
(All Cross Terms are Zero, Kxx=Kyy=495 lbf/in,Cxx=Cyy=0.04 lbf-sec/in).
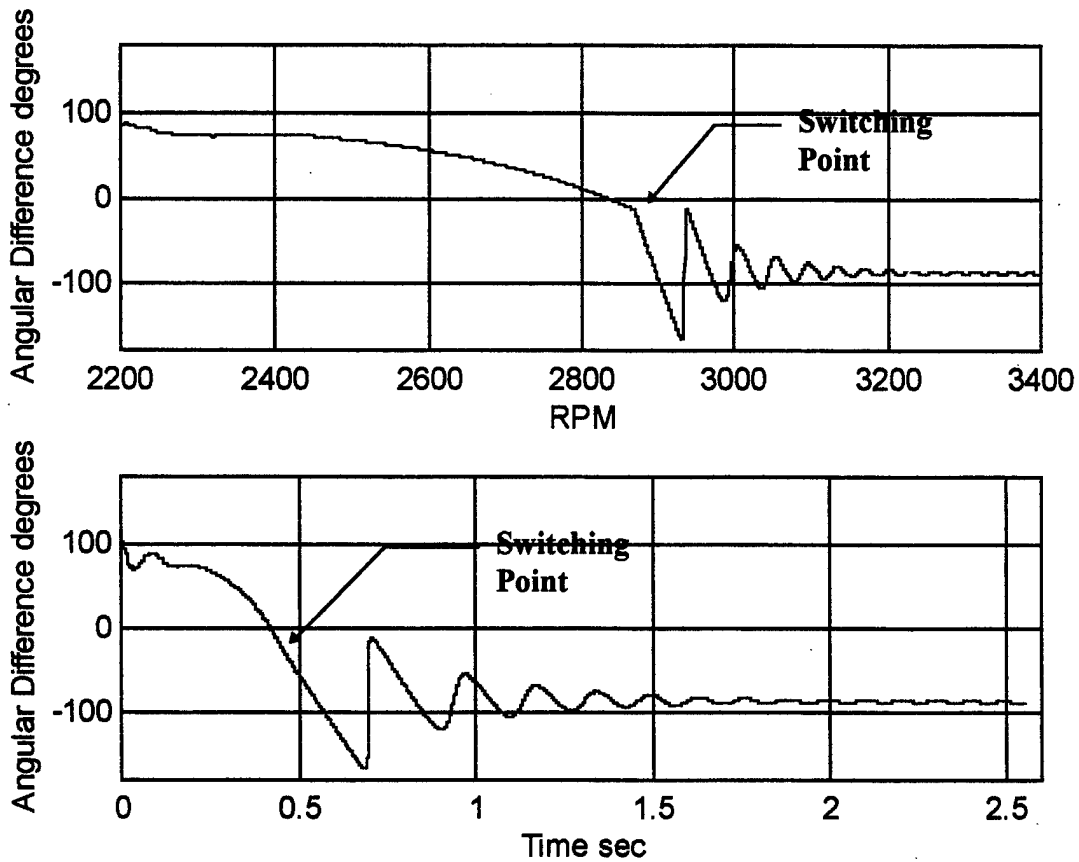
**Figure 18. Angle Between Force and Velocity Vectors of a Rotor.
Acceleration Schedule 2000 to 250 RPM/Sec at 2870 RPM
(All Cross Terms are Zero, Kxx=Kyy=495 lbf/in,Cxx=Cyy=0.04 lbf-sec/in).**
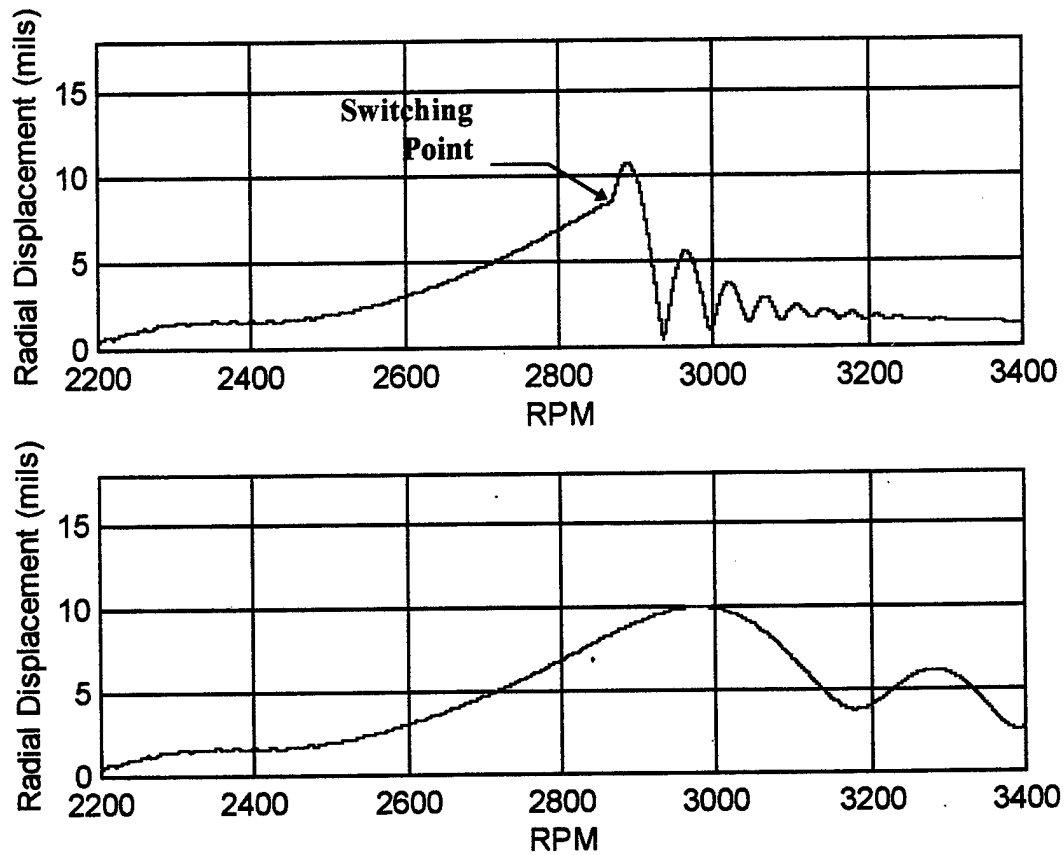
Figure 19. Radial Displacement Comparison
Acceleration Schedule (Upper Plot)   to
Constant High Acceleration Rate (2000 RPM/Sec) (Lower Plot) .
Acceleration Schedule 2000 to 250 RPM/Sec at 2870 RPM
(All Cross Terms are Zero, Kxx=Kyy=495 lbf/in,Cxx=Cyy=0.04 lbf-sec/in).

38

Figure 20. Radial Displacement Comparison
Acceleration Schedule (Upper Plot) to
Constant High Acceleration Rate (2000 RPM/Sec) (Lower Plot) .
Acceleration Schedule 2000 to 250 RPM/Sec at 2870 RPM
(All Cross Terms are Zero, Kxx=Kyy=495 lbf/in,Cxx=Cyy=0.04 lbf-sec/in).

39

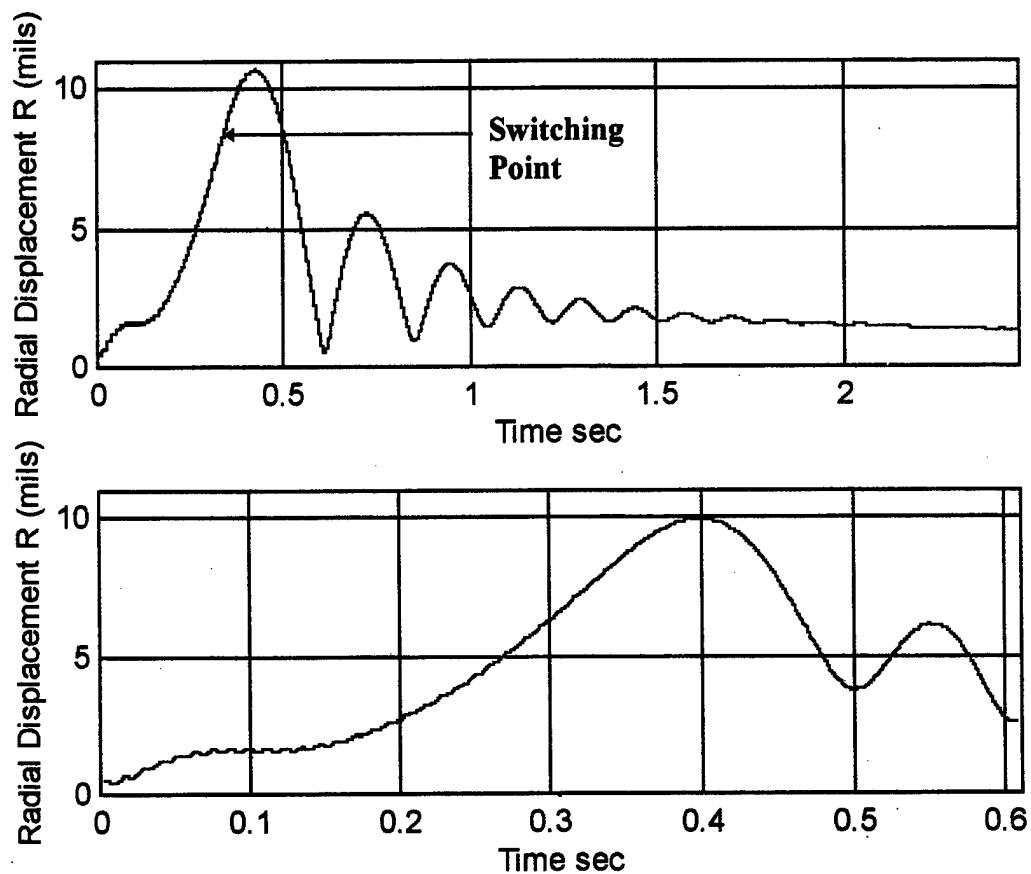# V. SUMMARY, CONCLUSIONS AND RECOMMENDATIONS

A. SUMMARY

An analytical model was developed to predict the response of a simple rotor with an arbitrary input acceleration. A study was conducted to determine the possibility of minimizing the maximum lateral bending response by acceleration scheduling. Although the study did not yield the anticipated positive results theorized, it did provide insight into the mechanics of the lateral bending response in this region.

B. CONCLUSIONS

The simple acceleration schedule of switching from a high to a low acceleration did not reduce the maximum amplitude of lateral vibrations. The acceleration schedule used in the model produced a higher amplitude than the constant high acceleration by 6%.

The analytical model predicted that acceleration scheduling reduces the amplitude and number of high lateral bending cycles in the supercritical speed region. The mean amplitude of the radial displacement is 62% less for the acceleration schedule response than that of the constant high acceleration response.

The rotation of the mass imbalance relative to the instantaneous disk velocity is a function of the imposed acceleration schedule. The angle between the mass imbalance and the instantaneous velocity of the disk does not exceed 180° until the rotor is supercritical.

Above the apparent critical speed, stabilization of the angular difference between the mass imbalance and the velocity vector at 180 ° is necessary for the amplitude of the radial displacement to diminish.

41

C. RECOMMENDATIONS

1.   Experimentally Verify the Results of Acceleration Scheduling.

The predictive capabilities of the model should be experimentally verified. The rotor kit should be modified such that the phase angle of the mass imbalance relative to the position and velocity of the rotor can be measured.

In addition to the measurement upgrade, the rotor kit would require a motor controller that would take electronic commands from a computer. This would be necessary to achieve an acceleration schedule. The computer implemented acceleration schedule would provide reliable and repeatable results.

2.   Generalize Results

The results obtained were specifically for the parameters of the rotor kit. A theoretical study should be conducted that would use the dimensionless parameters of Lewis [Ref. 2] and Gluse [Ref. 4]. Using Lewis' dimensionless acceleration and frequency and Gluse's dimensionless parameter for imbalance, stiffness and damping, a general description of the accelerating rotor could be obtained. The study could reveal the values of acceleration needed for a supercritical rotor to stabilize the phase angle of the mass imbalance of 180°.

APPENDIX

Table 1. List of specifications of the rotor kit used for the computer model.

Modal Mass of the disk (M) .... 0.00061 lbf-sec-sec/in

Mass of the eccentricity (m).......................... 0.0000057075 lbf-sec-sec/in (1 gram)

Eccentricity (e).. 1.2 in

Stiffness (Kxx) .... 495 lbf/in

Stiffness (Kyy).. 495 lbf/in

Damping (Cxx).. 0.04 lbf-sec/in (ζ=0.0115)

Damping (Cyy).. 0.04 lbf-sec/in (ζ=0.0115)

LIST OF REFERENCES

1. Reed, G.L., "Theoretical and Experimental Investigation of the Response of a Rotor Accelerating Through Critical Speed," Master's Thesis, Naval Postgraduate School, Monterey, California, December 1995.

2. Lewis, F.M., "Vibration During Acceleration Through a Critical Speed," Journal of Applied Mechanics, Trans. ASME, Vol 54, 1932.

3. Pöschl, "Das Anlaufen eines einfaches Schwingers", Ingenieur-Archiv, IV bd, p. 98, 1933.

4. Baker, J.G. "Mathematical-machine Determination of the Vibration of Accelerated Unbalanced Rotor", Journal of Applied Mechanics, Transactions of the ASME, Vol. 6 p. A1, 1939.

5. Meuser, R.B. and Weibel, E.E., "Vibration of a Nonlinear System During Acceleration Through Resonance," Journal of Applied Mechanics, Trans. ASME, Vol. 15, 1948.

6. McCann, Jr., G.D and Bennett, R.R. "Vibrations of Multifrequency Systems During Acceleration Through Critical Speeds," Journal of Applied Mechanics, Trans. ASME, Vol. 16, p. 375, 1949.

7. Filippov, A.P. "Vibrations of Elastic Systems," Academy of Sciences, Ukrainian SSR, Kiev. pp. 145-151, 1956.

8. Fearn, R.L. Milsaps, K., 1967, "Constant Acceleration of an Undamped Simple Vibrator Through Resonance," Journal of the Royal Aeronautical Society, p. 567, August 1967.

9. Gluse, M.R., "Acceleration of an Unbalanced Rotor Through its Critical Speeds," Naval Engineers Journal, pp. 135-144, February 1967.

10. Yamakawa, H. and Murakami, S., "Optimum Designs of Operating Curves for Rotating Shaft Systems with Limited Power Supplies", Current Topics in Structural Mechanics, Vol. 179, pp. 181-185, 1989.

11. Milsaps, K.T. and Reed, G.L., "Reducing Lateral Vibrations of a Rotor Passing Through Critical Speeds by Acceleration Scheduling" , ASME Presentation at the International Gas Turbine & Aeroengine Congress, June 1997.

INITIAL DISTRIBUTION LIST

1. Defense Technical Information Center 2
   8725 John J. Kingman Road, Ste 0944
   Ft. Belvoir, Virginia 22060-6218

2. Dudley Knox Library..2
   Naval Postgraduate School
   411 Dyer Road
   Monterey, California 93943-5101

3. Naval/Mechanical Engineering Curricular Officer, Code 34....................................1
   Naval Postgraduate School
   Monterey, California 93943-5101

4. Professor Knox T. Millsaps...4
   Mechanical Engineering Department, Code ME/KK
   Naval Postgraduate School
   Monterey, California 93943-5101

5. LT Cecil C. Bridges...2
   RT 1 Box 197
   Aldrich, Missouri 65601

6. Mr. Dan Grogan...1
   Director Engine Division, SEA-03X3
   NAVSEA HQ, NC4
   2341 Jefferson Davis Highway
   Arlington, Virginia 22242-5160

7. Mr. John Hartranf..1
   Manager LM-2500, SEA-03X34
   2341 Jefferson Davis Highway
   Arlington, Virginia 22242-5160